Efficient fully functionalized photorefractive polymethacrylates with infrared sensitivity and different spacer lengths

Christiaan Engels,[a] David Van Steenwinckel,[b] Eric Hendrickx,[b] Mark Schaerlaekens,[b] André Persoons[b] and Celest Samyn*[a]

[a]Laboratory of Macromolecular and Physical Organic Chemistry, University of Leuven, Celestijnenlaan 200F, B-3001 Leuven, Belgium. Tel: +32-(0)-16-327438; Fax: +32-(0)-16-327990; E-mail: celest.samyn@chem.kuleuven.ac.be (C. Samyn).
[b]Laboratory of Chemical and Biological Dynamics and Center for Research on Molecular Electronics and Photonics, University of Leuven, Celestijnenlaan 200D, B-3001 Leuven, Belgium

A series of photorefractive polymethacrylates, containing a Disperse Red type chromophore and carbazole as charge transport agent with various spacer lengths, was synthesized and characterized. The photorefractive effect of these materials was studied by four-wave mixing and two beam-coupling at 780 nm after sensitization with 1 wt% TNFM. We have found a gain coefficient of $\Gamma = 140$ cm^{-1} at an applied electric field of 60 V μm^{-1} and complete internal diffraction at an applied electric field of 52 V μm^{-1}. For fully functionalized photorefractive polymers, these values rank among the highest reported up to date.

Introduction

Photorefractive polymers are a recently discovered class of materials for dynamic holography, that combine the intrinsic advantages of polymers, such as synthetic flexibility, with excellent optical characteristics, such as high diffraction efficiencies and sub-second response times.[1–3] In a photorefractive polymer, charges that are generated by the absorption of light from an optical interference pattern, migrate under the influence of an externally applied electric field, until they are trapped. The resulting non-uniform charge distribution produces a so-called space-charge field. This space-charge field, in combination with the externally applied electric field, then modulates the polymer refractive index through birefringence and the Pockels effect. The components of a photorefractive polymer reflect the stepwise buildup of the index modulation, and include a small quantity of a charge generator, and large quantities of a charge transport molecule and a highly polar chromophore.

One way to combine all these properties in a single material is to mix a hole-transporting polymer, such as poly-(N-vinylcarbazole), with up to 50 wt% of a highly polar dye.[4] To enable chromophore reorientation, and thereby the enhancement of the index modulation amplitude *via* birefringence, the glass transition temperature is then further lowered to room temperature by the addition of N-ethylcarbazole as plasticizer. Such an approach can be convenient, since all the components can be readily purified and many different combinations can easily be tested. However, this approach will mostly produce mixtures that are thermodynamically unstable and show phase separation upon storage. The phase stability has been improved by using mixtures of chromophores,[5,6] but it is clear that for the complete elimination of phase separation fully functionalized polymers are the key to success and several synthetic approaches have been published in the literature.[7–10]

In previous work, we have reported on the synthesis and the photorefractive response of a series of functionalized methacrylate copolymers, where the carbazole and polar dye unit were covalently attached to the polymethacrylate backbone with n-hexyl spacers. In order to reduce the glass transition temperature, 20 mol% of dodececyl methacrylate was incorporated into the polymer.[11,12] This general polymer architecture is shown in Fig. 1(a). These polymers were the first fully functionalized polymers to show a net two-beam coupling gain at the infrared wavelength of 780 nm.

Here we report on the synthesis and photorefractive response of a similar series of copolymers **P1–P9**, shown in Fig. 1(b), wherein the spacer length between the pendant carbazole and dye units and the polymer backbone was varied to optimize the glass transition temperature and avoid the addition of external plasticizers. As the chromophore moiety, we have chosen the traditional azo-dye Disperse Red. The main goal of this new approach is to further increase the index modulation amplitude attainable in the copolymers. The elimination of the internal plasticizer can result in a larger chromophore number density. Furthermore, the Disperse Red dye has a larger dipole moment than the previously used 4,4′-dimethylaminonitrostilbene (DANS) chromophore, 8.1 D *versus* 6.6 D. We expect both factors to contribute to a larger dynamic range in this type of newly synthesized copolymers.

First, we discuss the polymer synthesis, characterization, and the variation of the polymer glass transition temperature with spacer length, followed by the sample preparation. Finally, the experimental setup and the photorefractive parameters of two of the copolymers, sensitized for infrared wavelengths by adding 1 wt% of (2,4,7-trinitrofluoren-9-ylidene)malononitrile (TNFM), are discussed. In these polymers and at a wavelength of 780 nm, we have observed internal diffraction efficiencies of 100% at applied fields as low as 52 V μm^{-1}. This photorefractive performance is among the best reported for infrared-sensitive fully functionalized polymers thus far.

Results and discussion

Synthesis of the photorefractive polymethacrylates

Hydroxyalkylcarbazoles **7–9** and hydroxyalkyl chromophores **12** and **13** were synthesized as presented in Schemes 1 and 2. They were reacted with methacryloyl chloride to yield the necessary monomers. Scheme 3 depicts the monomer and
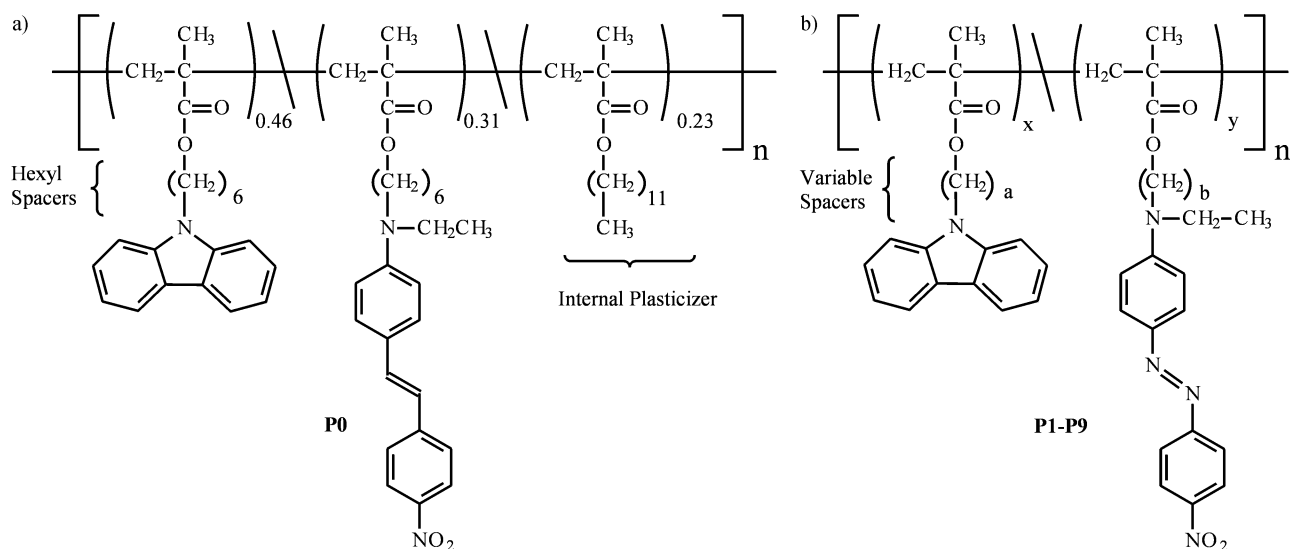
Fig. 1 Generalized structures of the copolymers previously characterized in ref. 11, **P0** (left), and the newly synthesized copolymers **P1**–**P9**. Note the use of a chromophore with higher polarity and the omission of the internal plasticizer and the variable spacer length.

polymer syntheses. The polymers were obtained by radical copolymerization of a carbazole- and chromophore-methacrylate in a 50 : 50 ratio. The polymerizations were carried out in *N,N*-dimethylformamide (DMF) at 65 °C for 24 h using 1 wt% of 2,2′-azobisisobutyronitrile (AIBN) as initiator under an argon atmosphere.

The compositions of the copolymers were determined by ^{1}H-NMR and are listed in Table 1. The results were consistent with the monomer feed. In Fig. 2, the ^{1}H-NMR spectrum of polymer **P7** is given. In NMR, it is well known that efficient relaxation results in broad peaks. This efficient relaxation is also observed in polymers, because of their high molecular weight compared to small molecules.[13] The ^{1}H-NMR spectra of **P1**–**P9** show a similar feature: they reflect well the influence of the spacer length on the mobility of the different moieties. A short spacer results in broader NMR peaks because of efficient relaxation. As the spacer length increases, the peaks become sharper and multiplets are better resolved.

The physical properties of polymers **P1**–**P9** are listed in Table 2. High yields and reasonable molecular weights were obtained and the GPC measurements showed a monomodal distribution for all polymers. As expected, the T_g decreases with increasing spacer length. This spacer creates a distance between the 'bulky' carbazole and chromophore groups, and the polymer backbone. This results in a more flexible polymer backbone and, hence a lower T_g.

Sample preparation

Samples for photorefractive measurements were prepared by dissolving the polymer in chloroform, and by adding TNFM up to 1 wt% concentration. After passing this solution through a 0.2 μm PTFE membrane filter, the solvent was allowed to evaporate for 3 hours at 80 °C. The resulting homogeneous mixture was then molten between two ITO-coated glass slides, and the thickness of the samples was controlled by glass spacers of 125 μm diameter.

For our optical experiments, we focus on two of the copolymers with a low T_g, **P6** and **P8**. Good quality optical films of these polymers could be prepared without adding plasticizer. Unfortunately, we were not able to prepare films of **P1**–**P4** without adding a plasticizer. More work is in progress to prepare films of good optical quality of the remaining polymers.
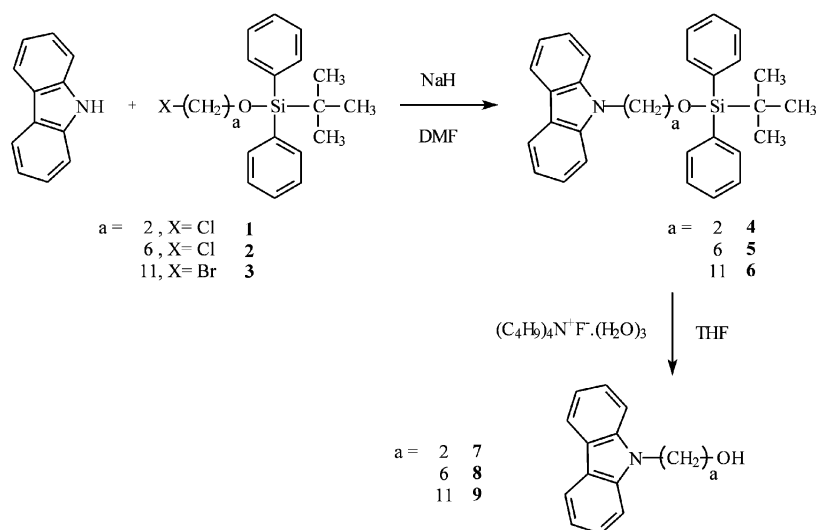
Scheme 1 Synthesis of hydroxyalkyl carbazoles **7**–**9**.
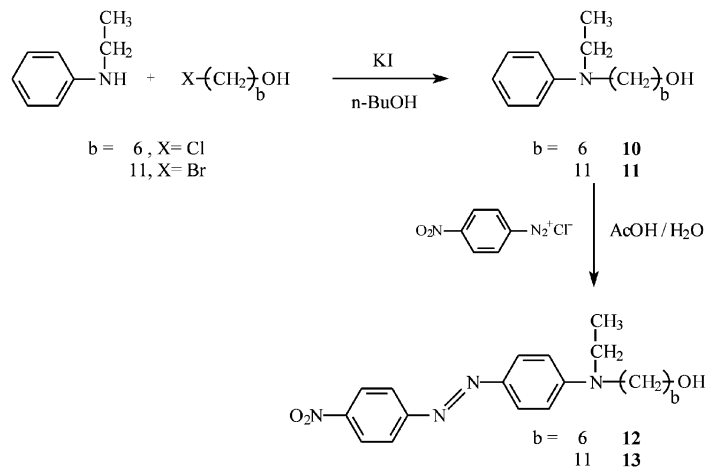
Scheme 2 Synthesis of hydroxyalkyl chromophores **12** and **13**.
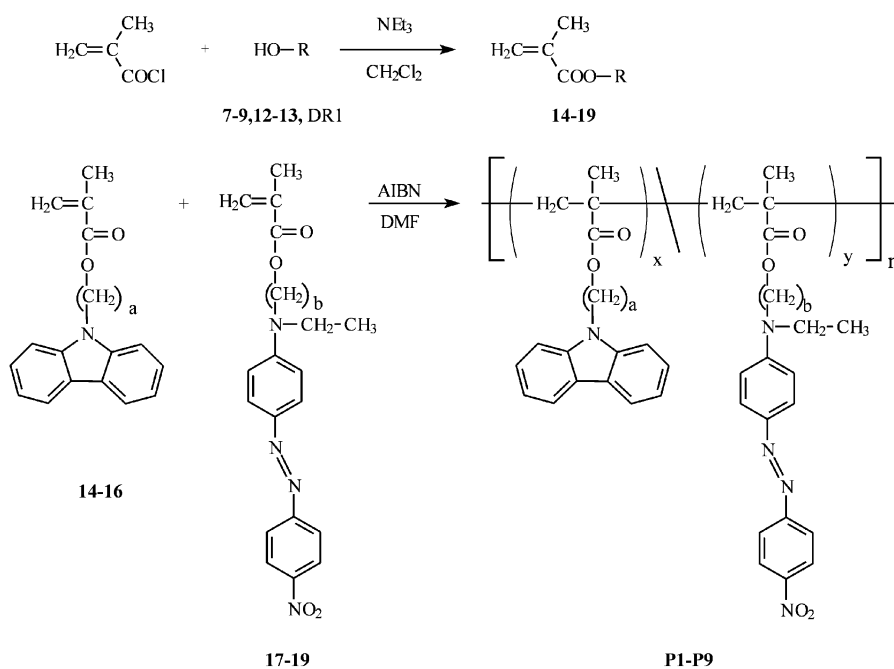
Scheme 3 Synthesis of monomers **14–19** and copolymers **P1–P9**.
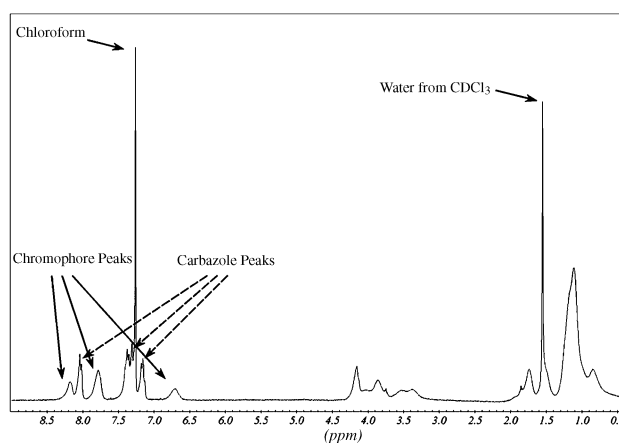
Photorefractive experiments

Two-beam coupling experiments and four-wave mixing experiments were done with a setup similar to the one described in reference.[14] All data were taken under steady state conditions and were reproducible within 5% of the experimental values. The laser was a diode laser operating at a wavelength of 780 nm. The angle between the two writing beams outside the samples was $(14 \pm 1)°$, and the angle between the bisector and the surface normal was $(50 \pm 2)°$. For

Table 1 Copolymerization results: composition and yield

Polymer	Spacer a/b^a	Composn. x/y^b	Yield (%)
P1	2/2	0.46/0.54	67
P2	2/6	0.52/0.48	95
P3	2/11	0.51/0.49	88
P4	6/2	0.45/0.55	71
P5	6/6	0.51/0.49	91
P6	6/11	0.53/0.47	86
P7	11/2	0.48/0.52	67
P8	11/6	0.55/0.45	91
P9	11/11	0.49/0.51	83

$^a a$ stands for the spacer length of the carbazole while b indicates the spacer length of the chromophore groups. $^b x$ stands for the mole fraction of the carbazole groups, while y indicates the chromophore mole fraction, measured by ^{1}H-NMR.

Fig. 2 ^{1}H-NMR of polymer **P7** in CDCl$_3$. The chromophore peaks are broader than the carbazole peaks due to the longer carbazole spacer.

Table 2 Physical properties of the copolymers **P1–P9**

Polymer	$\bar{M}_n$/g mol^{-1a}	$\bar{M}_w$/g mol^{-1a}	$\bar{M}_w/\bar{M}_n{}^b$	T_g/°C
P1	13 700	47 100	3.4	131 ± 2
P2	19 400	78 000	4.0	100 ± 2
P3	27 000	95 700	3.5	60 ± 2
P4	10 000	31 000	3.1	87 ± 2
P5	21 500	56 200	2.6	74 ± 2
P6	25 000	75 500	3.0	33 ± 2
P7	13 800	42 000	3.0	51 ± 2
P8	32 600	72 000	2.2	38 ± 2
P9	28 500	113 000	4.0	36 ± 2

^{a}Apparent molecular weights measured by GPC in THF, polystyrene standards. ^{b}Polydispersity.

the two-beam coupling experiments, the two beams were p-polarized, had a power of 2.8 ± 0.1 mW each, and were collimated to (250 ± 10) μm diameter in the sample. The analysis of the data was done using eqn. (1),

$$\Gamma d = \cos\alpha_1\left(\ln\frac{I_1^t(I_2\neq0)}{I_1^t(I_2=0)}\right) - \cos\alpha_2\left(\ln\frac{I_2^t(I_1\neq0)}{I_2^t(I_1=0)}\right) \quad (1)$$

where I_1^t and I_2^t are the transmitted intensities of writing beams 1 and 2. Beam 1 is the beam closest to the surface normal, α_1 and α_2 are the angles between the writing beams and the surface normal in the sample, d is the sample thickness, and Γ is the gain coefficient.

Four-wave mixing experiments were performed using s-polarized writing beams, and a p-polarized probe beam, counterpropagating to writing beam 1. The power of the writing beams was the same as in the two-beam coupling experiments, and the probe beam, collimated to (150 ± 10) μm, had a power of (2.0 ± 0.1) μW. The internal diffraction efficiencies were calculated using the formula

$$\eta_{int} = \frac{I_{diff}}{I_t} \quad (2)$$

where I_{diff} is the intensity of the light diffracted upon the photorefractive grating, and I_t is the total amount of light transmitted through the sample, that is, the sum of the diffracted and transmitted intensities.

Photorefractive parameters

The internal diffraction efficiencies measured for 125 μm thick samples of polymers **P6** and **P8** as a function of applied electric field are shown in Figs. 3a and 3b, respectively. The optical wavelength was 780 nm, and the experiments were conducted at T_g +2 °C, or at 35 °C and 40 °C for polymers **P6** and **P8**, respectively. The insets in Figs. 3a and 3b show the absorption spectra of 125 μm thick samples of the pure polymers and the polymers sensitized with 1 wt% of TNFM. For a poly(N-vinylcarbazole) sample sensitized with TNFM, a charge-transfer complex is formed between carbazole and TNFM.[15] This complex absorbs in the wavelength range of 600–850 nm and this absorption decreases rapidly beyond 830 nm. The fact that the absorption in polymers **P6** and **P8** extends beyond 900 nm is indicative of an additional complexation occurring between the chromophore and TNFM. We have experimentally determined the stability constants and molar absorption coefficients of the two complexes by applying the Benesi–Hildenbrandt equation[16] to the optical density changes in a dilution series of the complex in a poly(methyl methacrylate) polymer film. N-Ethylcarbazole (ECZ) was used as a model compound for poly(N-vinylcarbazole). The analysis showed that the chromophore–TNFM complex has a smaller complexation constant ($K = 0.30$ M^{-1} vs. $K = 2.6$ M^{-1}) but a larger molar absorptivity at 780 nm than the ECZ–TNFM complex (2100 M^{-1} cm^{-1} vs. 260 M^{-1} cm^{-1}). Extrapolation of these data to the TNFM-sensitized copolymer implies that 10 times
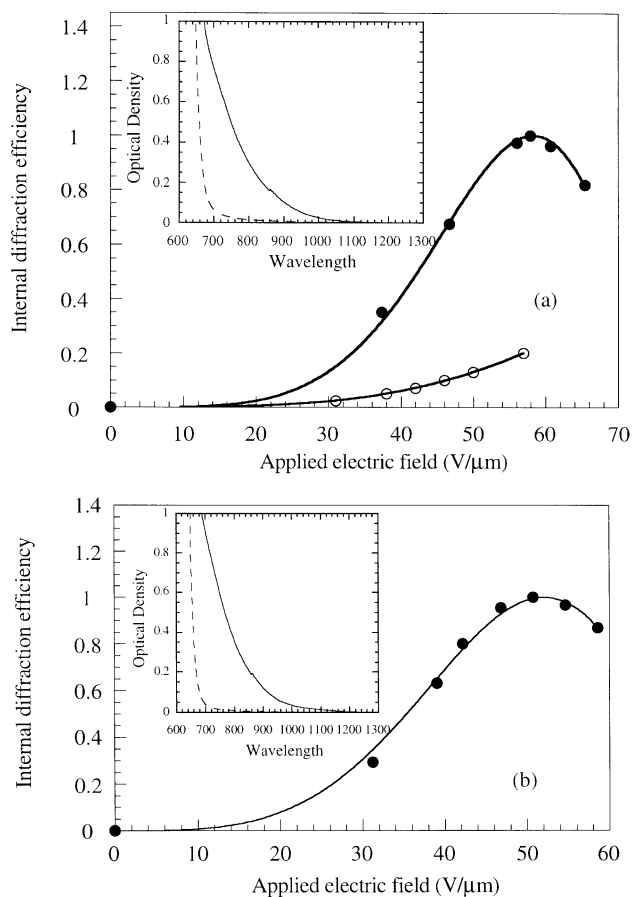
Fig. 3 (a): Internal diffraction efficiency as a function of applied electric field for polymer **P6** (filled circles) and the copolymer with internal plasticizer **P0** at T_g +2 °C. Inset: Absorption spectrum of a sample of polymer **P6** with (full lines) and without 1 wt% of TNFM sensitizer. (b) Internal diffraction efficiency as a function of applied electric field for polymer **P8**. Inset: Absorption spectrum of a sample of polymer **P8** with (full lines) and without 1 wt% of TNFM sensitizer. All samples were 125 μm thick, were measured at T_g +2 °C and at a wavelength of 780 nm. All curves are fits to the general equation.

more carbazole–TNFM complexes are present than chromophore–TNFM complexes, but because of their higher molar absorptivity the latter still absorb 50% of the incoming light.

As can be seen from the curve fits in both figures, the internal diffraction efficiency follows the typical dependence of the applied field that is expected from the theory of Kogelnik for slanted gratings:[17]

$$\eta_{int} = sin^2(C\Delta n) \quad (3)$$

where C is a constant that depends on the experimental geometry ($C = 564$ in our experimental geometry) and the index modulation amplitude Δn varies with the applied electric field E_{Ext} according to:

$$\Delta n = N(A\mu^2\Delta\alpha + B\mu\beta)E_{Ext}E_{Sc} \quad (4)$$

Here various constants are combined in A and B, such as the local field and geometry factors. μ is the molecular dipole moment, $\Delta\alpha$ the polarizability anisotropy, β the first hyperpolarizability and N the number density of chromophores. E_{Sc} is the amplitude of the space charge field that is directly proportional to the amplitude of the applied electric field if the space-charge field is completely saturated.

In Fig. 3a, the internal diffraction efficiency of **P0** (in Fig. 1a) at T_g +2 °C (open circles) is plotted together with that of polymer **P6** (filled circles). A clear improvement of the internal diffraction efficiency can be observed. A calculation of the index modulation amplitude at an applied field of 58 V μm^{-1}
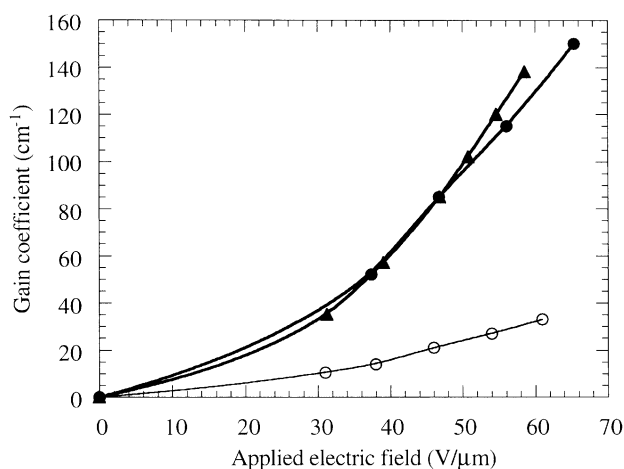
using eqn. (3) shows that Δn is three times larger for polymer **P6** (2.8×10^{-3} vs. 8.4×10^{-4}, respectively). According to eqn. (4), this enhancement can in part be attributed to a larger chromophore number density and chromophore dipole moment in polymer **P6** ($N = 7.5 \times 10^{20}$ cm^{-3} and $\mu = 8.1$ D for **P6**,[18] vs. $N = 5.9 \times 10^{20}$ cm^{-3} and $\mu = 6.6$ D for the polymer with the internal plasticizer). Similar diffraction efficiencies for polymers **P6** and **P8** in Figs. 3a and 3b could be foreseen, since the chromophores, and thus the molecular dipole moments, are identical and the chromophore number densities are similar for the two polymers ($N = 7.1 \times 10^{20}$ cm^{-3} for **P8**). It also implies that both the hexyl and undecyl spacers are flexible enough to allow the chromophores to reorient to their equilibrium positions within the timescale of the experiment. The overmodulation of the diffraction efficiency observed at fields of 58 and 52 V μm^{-1} places these materials among the most efficient infrared-sensitive functionalized polymers reported to date.

The results of the asymmetric two-beam coupling are shown in Fig. 4. The filled symbols stand for the two-beam coupling gain coefficients Γ of polymers **P6** and **P8** as a function of applied electric field. This coefficient is related to the index modulation amplitude by:

$$\Gamma = \frac{4\pi}{\lambda}(\bar{e}_1\bar{e}_2^*)\Delta n \sin\theta \qquad (5)$$

where λ is the optical wavelength, $\bar{e}_1$ and $\bar{e}_2$ are the polarization vectors of the two writing beams, and θ is the photorefractive phase shift between the space-charge field and the interference pattern generated by the interacting beams. Since both polymers **P6** and **P8** have similar index modulation amplitudes Δn and gain coefficients, it follows from eqn. (5) that they also have comparable photorefractive phase shifts. The open symbols in Fig. 4 are the gain coefficient of **P0**. Note the clear improvement in gain coefficient by a factor of ~ 4. From eqn. (5), and the experimental diffraction efficiencies, it is clear that the enhancement of the index modulation amplitude by a factor of 3 is the main factor leading to the improved gain coefficient. Although higher values of gain coefficients have been reached for blends[19] and guest–host systems,[20,21] a value of 140 cm^{-1} at an applied field of 60 V μm^{-1} and at a fundamental wavelength of 780 nm ranks among the highest values reported thus far for fully functionalized polymers without the addition of external plasticizers.

All data points were taken at steady state conditions, which was reached after several tens of seconds. Clearly, the slow nature of the grating build-up is a drawback of these materials.

Both the diffraction efficiency and gain coefficient of the two copolymers are significantly larger than the diffraction efficiency (1% at 100 V μm^{-1}) and gain coefficient (7 cm^{-1} at 100 V μm^{-1}) reported for a poly([2-(N-ethyl-N-{4-[2-(4'-nitrophenyl)ethenyl]phenyl}amino)ethyl]-co-[2-(carbazol-9-yl)-ethyl]-co-[n-octyl]) methacrylate.[22] This difference can be attributed to several factors. First, the chromophore only constituted 17 mol% of the copolymer units. In addition, the chromophore was identical to that used in **P0**, and thus had a small dipole moment. Finally, in ref. 22 the optical experiments were done at room temperature, whereas the polymer T_g was 47 °C. In previous work, we have shown that the enhancement of the index modulation amplitude by birefringence is virtually absent on the timescale of a photorefractive experiment at T_g −20 °C, and is fully operational at T_g −5 °C.[23] This again shows the importance of the careful optimization of the polymer glass transition temperature by adjusting the spacer length.

Conclusion

In conclusion, we have synthesized a new series of infrared-sensitive photorefractive polymethacrylates functionalized with carbazole and a polar chromophore. No internal plasticizer was used, but the spacer lengths were varied to reduce the glass transition temperature. A glass transition temperature close to room temperature was observed for the copolymers with hexyl and undecyl spacer lengths. Four-wave mixing and two-beam coupling experiments conducted at 780 nm showed excellent photorefractive properties, with gain coefficients exceeding 150 cm^{-1} and complete internal diffraction at a field of 52 V μm^{-1}. The only drawback here is the slow grating formation of these materials. The improvement of the photorefractive response of these polymers compared to a previously synthesized copolymer with internal plasticizer is attributed to the higher polarity and number density of the pendant chromophore.

Experimental

General methods

All reagents are commercially available and used as received unless stated otherwise. All synthesized products and polymers were characterized by a Bruker Avance 300 (300 MHz) ^{1}H-NMR. The molecular weights were determined by gel permeation chromatography (Waters HP/GPC), using THF as eluent and toluene as internal reference; polystyrene standards were used for calibration. The glass transition temperatures (T_g) of the polymers were measured by differential scanning calorimetry (DSC), using a Perkin-Elmer DSC-7. All samples were heated at a rate of 20 °C min^{-1}. The listed T_g's were measured after a second heating run.

Silylation of the alcohol group with tert-butyldiphenylsilyl chloride. General procedure.[24]

To a mixture of 0.09 mol of the halogenated alcohol and 13.5 g (0.198 mol) of imidazole in 100 mL of dry DMF, 25.7 mL (0.099 mol) of tert-butyldiphenylsilyl chloride is added dropwise and stirred for 4 h at room temperature. The reaction mixture is poured into water, extracted with diethyl ether, the organic phase dried (MgSO$_4$) and the solvent removed under reduced pressure to yield the protected halogenated alcohols **1-3**. These products were obtained as a slightly yellow oil and were pure enough to be used in the next step.

Fig. 4 Gain coefficients as a function of applied electric field for polymers **P6** (filled circles), **P8** (filled triangles) and the copolymer with internal plasticizer (open circles) **P0**. All samples were 125 μm thick, were measured at T_g +2 °C and at a wavelength of 780 nm. The solid lines are guides to the eye.

2-(*tert*-Butyldiphenylsilyloxy)ethyl chloride (1). Yield: 27.6 g (96%). ^{1}H-NMR (CDCl$_3$, ppm) δ = 7.7 (d, 4H), 7.4 (m, 6H), 4.0 (t, 2H), 3.6 (t, 2H), 1.1 (s, 9H).

6-(*tert*-Butyldiphenylsilyloxy)hexyl chloride (2). Yield: 33.4 g (99%). ^{1}H-NMR (CDCl$_3$, ppm) δ = 7.7 (d, 4H), 7.4 (m, 6H), 3.7 (t, 2H), 3.5 (t, 2H), 1.7 (m, 2H), 1.6 (m, 2H), 1.4 (m, 4H), 1.1 (s, 9H).

11-(*tert*-butyldiphenylsilyloxy)undecyl bromide (3). Yield: 42.5 g (96%). ^{1}H-NMR (CDCl$_3$, ppm) δ = 7.7 (d, 4H), 7.4 (m, 6H), 3.7 (t, 2H), 3.5 (t, 2H), 1.75 (m, 2H), 1.55 (m, 2H), 1.4–1.2 (m, 14H), 1.1 (s, 9H).

Synthesis of the *N*-alkylated carbazole derivatives. General procedure

To a solution of 12 g (0.072 mol) of carbazole and 0.6 g (4.0 mmol) of NaI in 100 mL of dry DMF, a dispersion of 1.9 g (0.079 mol) of NaH in 30 mL of dry DMF is added dropwise. After 1 h of stirring, 0.079 mol of protected halogenated alcohol **1–3** dissolved in 20 mL of dry DMF is added dropwise. The reaction mixture is then heated to 65 °C for 24 h, cooled, poured into water and extracted with CH$_2$Cl$_2$. The organic layer is dried (MgSO$_4$) and the solvent removed under reduced pressure. Finally, the products **4–6** are purified by column chromatography (silica gel).

9-[2-(*tert*-Butyldiphenylsilyloxy)ethyl]carbazole (4). Eluent: CH$_2$Cl$_2$. Yield: 22.8 g (63%) of a slightly yellow oil. ^{1}H-NMR (CDCl$_3$, ppm) δ = 8.1 (d, 2H), 7.6–7.2 (m, 16H), 4.4 (t, 2H), 4.0 (t, 2H), 1.0 (s, 9H).

9-[6-(*tert*-Butyldiphenylsilyloxy)hexyl]carbazole (5). Eluent: CH$_2$Cl$_2$–CH$_3$CN 90 : 10 v/v. Yield: 16.4 g (45%) of a slightly yellow oil. ^{1}H-NMR (CDCl$_3$, ppm) δ = 8.1 (d, 2H), 7.6 (d, 4H), 7.5–7.3 (m, 10H), 7.2 (m, 2H), 4.3 (t, 2H), 3.6 (t, 2H), 1.8 (m, 2H), 1.5–1.2 (m, 6H), 1.0 (s, 9H).

9-[11-(*tert*-Butyldiphenylsilyloxy)undecyl]carbazole (6). Eluent: CH$_2$Cl$_2$–*n*-hexane 90 : 10 v/v. Yield: 19.2 g (46%) of a slightly yellow oil. ^{1}H-NMR (CDCl$_3$, ppm) δ = 8.1 (d, 2H), 7.6 (d, 4H), 7.5–7.3 (m, 10H), 7.2 (m, 2H), 4.3 (t, 2H), 3.6 (t, 2H), 1.8 (m, 2H), 1.5 (m, 2H), 1.4–1.2 (m, 14H), 1.0 (s, 9H).

Removal of the *tert*-butyldiphenylsilyl protective group. General procedure.[24]

A mixture of 0.032 mol of protected carbazole derivative (**4–6**) and 20.2 g (0.064 mol) of tetrabutylammonium fluoride·trihydrate in 120 mL of THF is stirred for 24 h at room temperature. To the concentrated reaction mixture, CH$_2$Cl$_2$ is added, and washed with water, the organic layer is dried (MgSO$_4$) and the solvent removed under reduced pressure. The products are then purified by column chromatography (silica gel).

9-(2-Hydroxyethyl)carbazole (7). Eluent: CH$_2$Cl$_2$. Yield: 4.2 g (62%), mp 85.5–87.3 °C. ^{1}H-NMR (CDCl$_3$, ppm) δ = 8.1 (d, 2H), 7.4 (m, 4H), 7.2 (m, 2H), 4.3 (t, 2H), 3.6 (t, 2H)

9-(6-Hydroxyhexyl)carbazole (8). Eluent: CH$_2$Cl$_2$–CH$_3$CN 90 : 10 v/v. Yield: 5.4 g (63%), mp 125.7–127.0 °C. ^{1}H-NMR (CDCl$_3$, ppm) δ = 8.1 (d, 2H), 7.4 (m, 4H), 7.2 (m, 2H), 4.3 (t, 2H), 3.6 (t, 2H), 1.8 (m, 2H), 1.5–1.2 (m, 6H).

9-(11-Hydroxyundecyl)carbazole (9). Eluent: CH$_2$Cl$_2$. Yield: 6.9 g (64%), mp 73.8–74.6 °C. ^{1}H-NMR (CDCl$_3$, ppm) δ = 8.1 (d, 2H), 7.4 (m, 4H), 7.2 (m, 2H), 4.3 (t, 2H), 3.6 (t, 2H), 1.8 (m, 2H), 1.6 (m, 2H), 1.5–1.2 (m, 14H).

N-Ethyl-N-(6-hydroxyhexyl)aniline (10). Compound **10** was prepared as described in a previous paper.[11] Yield: 26.2 g (72%), bp 167 °C (1.5 mmHg). ^{1}H-NMR (CDCl$_3$, ppm) δ = 7.2 (m, 2H), 6.8 (m, 3H), 3.6 (m, 2H), 3.2 (m, 4H), 2.9 (br s, 1H), 1.3 (m, 8H), 1.1 (t, 3H).

N-Ethyl-N-(11-hydroxyundecyl)aniline (11). Compound **11** was prepared according to Heldmann and Warner.[25] Yield: 9.5 g (79%), bp 183–185 °C (0.1 mmHg). ^{1}H-NMR (CDCl$_3$, ppm) δ = 7.2 (m, 2H), 6.8 (m, 3H), 3.6 (m, 2H), 3.2 (m, 4H), 1.6 (m, 4H), 1.3 (m, 14H), 1.1 (t, 3H).

Synthesis of the chromophores 12 and 13. General procedure.[26]

To a cooled (0–5 °C) solution of 16.3 g (0.12 mol) of *p*-nitroaniline in 120 mL of a 1 : 2 v/v mixture of HCl–water, a solution of 9.0 g (0.13 mol) of NaNO$_2$ in 18 mL of water is added dropwise. After formation of the diazonium salt, 0.12 mol of the aniline derivative (**10** and **11**) in 25 mL of acetic acid is added dropwise under stirring. The mixture is stirred for 30 min and a solution of 9.0 g (0.11 mol) of sodium acetate in 20 mL of water is added. After 1 h, another 9.0 g (0.11 mol) of sodium acetate in 20 mL of water is added. The mixture is then warmed up to room temperature and neutralized with a NaOH solution. After filtration, the crude product is purified by column chromatography (silica gel).

N-Ethyl-N-[4-(4-nitrophenylazo)phenyl]aminohexanol (12). Eluent: CHCl$_3$–CH$_3$CN 80 : 20 v/v. Yield: 25.5 g (58%), mp 110.0–110.5 °C. ^{1}H-NMR (CDCl$_3$, ppm) δ = 8.3 (d, 2H), 7.9 (m, 4H), 6.7 (d, 2H), 3.6 (m, 2H), 3.5 (q, 2H), 3.4 (t, 2H), 1.7–1.5 (m, 4H), 1.4–1.2 (m, 7H).

N-Ethyl-N-[4-(4-nitrophenylazo)phenyl]aminoundecanol (13). Eluent: CH$_2$Cl$_2$–CH$_3$CN 85 : 15 v/v. Yield: 9.2 g (69%), mp 71.5–72.7 °C. ^{1}H-NMR (CDCl$_3$, ppm) δ = 8.3 (d, 2H), 7.9 (m, 4H), 6.7 (d, 2H), 3.6 (m, 2H), 3.5–3.4 (m, 4H), 1.7–1.5 (m, 4H), 1.4–1.1 (m, 17H).

Monomer synthesis. General procedure.[27]

A mixture of 0.02 mol of one of the alcohols (**7–9**, **12**, **13** and Disperse Red 1), 4.0 g (0.04 mol) of triethylamine, 20 mg (0.18 mmol) of hydroquinone, and 150 mL of dichloromethane was cooled to 0 °C; 3.1 g (0.03 mol) of methacryloyl chloride in 15 mL of dichloromethane was added dropwise under stirring. The reaction was kept at 0–5 °C for 48 h under stirring, then washed with water. The organic layer was dried (MgSO$_4$) and the solvent removed under reduced pressure. The remaining reaction product was purified by column chromatography (silica gel) using dichloromethane as eluent.

2-(Carbazol-9-yl)ethyl methacrylate (14). Yield: 5.4 g (96%), mp 85.5–86.5 °C. ^{1}H-NMR (CDCl$_3$, ppm) δ = 8.1 (d, 2H), 7.5 (m, 4H), 7.3 (d, 2H), 6.1 (s, 1H), 5.9 (s, 1H), 4.4 (t, 2H), 4.2 (t, 2H), 1.9 (s, 3H).

6-(Carbazol-9-yl)hexyl methacrylate (15). Yield: 5.3 g (80%). ^{1}H-NMR (CDCl$_3$, ppm) δ = 8.1 (d, 2H), 7.5 (m, 4H), 7.3 (d, 2H), 6.1 (s, 1H), 5.9 (s, 1H), 4.3 (t, 2H), 4.1 (t, 2H), 1.9 (s, 3H), 1.5 (m, 4H), 1.4 (m, 4H).

11-(Carbazol-9-yl)undecyl methacrylate (16). Yield: 7.4 g (90%). ^{1}H-NMR (CDCl$_3$, ppm) δ = 8.1 (d, 2H), 7.5 (m, 4H), 7.3 (d, 2H), 6.1 (s, 1H), 5.9 (s, 1H), .4.3 (t, 2H), 4.1 (t, 2H), 1.9 (s, 3H), 1.6–1.5 (m, 4H), 1.4–1.2 (m, 14H).

2-{N-Ethyl-N-[4-(4-nitrophenylazo)phenyl]amino}ethyl methacrylate (17). Disperse Red 1 (DR1) was recrystallized from

ethanol before use. Yield: 6.6 g (87%), mp 103.2–104.0 °C. ^{1}H-NMR (CDCl$_3$, ppm) δ = 8.3 (d, 2H), 7.9 (m, 4H), 6.7 (d, 2H), 6.1 (s, 1H), 5.6 (s, 1H), 4.3 (t, 2H), 3.5 (q, 2H), 3.4 (t, 2H), 1.9 (s, 3H), 1.2 (t, 3H).

6-{*N*-Ethyl-*N*-[4-(4-nitrophenylazo)phenyl]amino}hexyl methacrylate (18). Yield: 7.9 g (90%), mp 62.0–62.4 °C. ^{1}H-NMR (CDCl$_3$, ppm) δ = 8.3 (d, 2H), 7.9 (m, 4H), 6.7 (d, 2H), 6.1 (s, 1H), 5.6 (s, 1H), 4.2 (t, 2H), 3.5 (q, 2H), 3.4 (t, 2H), 1.9 (s, 3H), 1.7 (m, 4H), 1.4 (m, 4H), 1.2 (t, 3H).

11-{*N*-Ethyl-*N*-[4-(4-nitrophenylazo)phenyl]amino}undecyl methacrylate (19). Yield: 8.3g (82%), mp 58.7–59.0 °C. ^{1}H-NMR (CDCl$_3$, ppm) δ = 8.3 (d, 2H), 7.9 (m, 4H), 6.7 (d, 2H), 6.1 (s, 1H), 5.6 (s, 1H), 4.2 (t, 2H), 3.5 (q, 2H), 3.4 (t, 2H), 1.9 (s, 3H), 1.7 (m, 4H), 1.4–1.2 (m, 17H).

Polymer synthesis. General procedure.[27]

The polymerizations were carried out in DMF solution under argon atmosphere at 65 °C in the presence of 1 wt% AIBN for 24 h. The resulting polymer solution was cooled and poured into methanol to precipitate the polymer. The precipitated polymer was filtered, redissolved and reprecipitated, filtered and finally dried under reduced pressure.

Acknowledgements

References

1 W. E. Moerner and S. M. Silence, *Chem. Rev.*, 1994, **94**, 127.
2 B. Kippelen, K. Meerholz and N. Peyghambarian, in *Nonlinear Optics of Organic Molecules and Polymers*, eds H. S. Nalwa and S. Miyata, Chemical Rubber Company, Boca Raton, FL, 1997, p. 465.
3 W. E. Moerner, A. Grunnet-Jepsen and C. L. Thompson, *Annu. Rev. Mater. Sci.*, 1997, **27**, 585.
4 K. Meerholz, B. L. Volodin, Sandalphon, B. Kippelen and N. Peyghambarian, *Nature*, 1994, **371**, 497.
5 E. Hendrickx, B. L. Volodin, D. D. Steele, J. L. Maldonado, J. F. Wang, B. Kippelen and N. Peyghambarian, *Appl. Phys. Lett.*, 1997, **71**, 1159.
6 K. Meerholz, R. Bittner, Y. De Nardin, C. Bräuchle, E. Hendrickx, B. L. Volodin, B. Kippelen and N. Peyghambarian, *Adv. Mater.*, 1997, **9**, 1043.
7 Z. Peng, A. R. Gharavi and L. Yu, *J. Am. Chem. Soc.*, 1997, **119**, 4622.
8 F. Wang, Z. Chen, Q. Gong, Y. Chen and H. Chen, *Solid State Commun.*, 1998, **108**(5), 295.
9 S.-H. Park, K. Ogino and H. Sato, *Polym. Adv. Technol.*, 2000, **11**, 349.
10 Y. Chen, Y. He, F. Wang, H. Chen and Q. Gong, *Polymer*, 2001, **42**, 1101.
11 D. Van Steenwinckel, C. Engels, E. Gubbelmans, E. Hendrickx, C. Samyn and A. Persoons, *Macromolecules*, 2000, **33**, 4074.
12 D. Van Steenwinckel, E. Hendrickx, C. Samyn, C. Engels and A. Persoons, *J. Mater. Chem.*, 2000, **10**, 2692.
13 D. H. Williams and I. Fleming, in *Spectroscopic Methods in Organic Chemistry*, (McGraw-Hill, London, 1995), p. 102.
14 B. L. Volodin, Sandalphon, K. Meerholz, B. Kippelen, N. V. Kukhtarev and N. Peyghambarian, *Opt. Eng.*, 1995, **34**, 2213.
15 E. Hendrickx, J. F. Wang, J. L. Maldonado, B. L. Volodin, Sandalphon, E. A. Mash, A. Persoons, B. Kippelen and N. Peyghambarian, *Macromolecules*, 1998, **31**, 734.
16 R. Foster, in *Organic Charge-Transfer Complexes*, Academic Press, London, 1969, p. 124.
17 H. Kogelnik, *Bell Syst. Tech. J.*, 1969, **48**, 2909.
18 C. R. Moylan, R. J. Twieg, V. Y. Lee, S. A. Swanson, K. M. Betterton and R. D. Miller, *J. Am. Chem. Soc.*, 1993, **115**, 12599.
19 J.-W. Lee and J.-K. Park, *Mol. Cryst. Liq. Cryst.*, 2000, **349**, 131.
20 I. K. Moon, D. Yoo, H. S. Moon, D.-H. Shin, W. S. Jahng, H. Chun and N. Kim, *Mol. Cryst. Liq. Cryst.*, 2000, **349**, 43.
21 D. Wright, M. A. Diaz-Garcia, J. D. Casperson, M. DeClue, W. E. Moerner and R. J. Twieg, *Appl. Phys. Lett.*, 1998, **73**(11), 1490.
22 C. Zhao, C.-K. Park, P. Prasad, Y. Zhang, S. Ghosal and R. Burzynski, *Chem. Mater.*, 1995, **7**, 1237.
23 D. Van Steenwinckel, E. Hendrickx, A. Persoons, K. Van den Broeck and C. Samyn, *J. Chem. Phys.*, 2000, **112**, 11030.
24 S. Hanessian and P. Lavallee, *Can. J. Chem.*, 1975, **53**, 2975.
25 C. Heldmann and M. Warner, *Macromolecules*, 1998, **31**, 3519.
26 C. Samyn, T. Verbiest, E. Kesters, K. Van den Broeck, M. Van Beylen and A. Persoons, *Polymer*, 2000, **41**, 6049.
27 P. Rondou, M. Van Beylen, C. Samyn, G. s'Heeren and A. Persoons, *Makromol. Chem.*, 1992, **193**, 3045.